Cardiac Hyaluronan Synthesis Is Critically Involved in the Cardiac Macrophage Response and Promotes Healing After Ischemia Reperfusion Injury

Anne Petz,* Maria Grandoch,* Daniel J. Gorski, Marcel Abrams, Marco Piroth, Rebekka Schneckmann, Susanne Homann, Julia Müller, Sonja Hartwig, Stefan Lehr, Yu Yamaguchi, Thomas N. Wight, Simone Gorressen, Zhaoping Ding, Sebastian Kötter, Martina Krüger, Andre Heinen, Malte Kelm, Axel Gödecke, Ulrich Flögel, Jens W. Fischer

Rationale: **Immediate changes in the ECM (extracellular matrix) microenvironment occur after myocardial ischemia and reperfusion (I/R) injury.**

Objective: **Aim of this study was to unravel the role of the early hyaluronan (HA)-rich ECM after I/R.**

Methods and Results: **Genetic deletion of *Has2* and *Has1* was used in a murine model of cardiac I/R. Chemical exchange saturation transfer imaging was adapted to image cardiac ECM post-I/R. Of note, the cardiac chemical exchange saturation transfer signal was severely suppressed by *Has2* deletion and pharmacological inhibition of HA synthesis 24 hours after I/R. *Has2* KO (*Has2* deficient) mice showed impaired hemodynamic function suggesting a protective role for endogenous HA synthesis. In contrast to *Has2* deficiency, *Has1*-deficient mice developed no specific phenotype compared with control post-I/R. Importantly, in *Has2* KO mice, cardiac macrophages were diminished after I/R as detected by ^{19}F MRI (magnetic resonance imaging) of perfluorcarbon-labeled immune cells, Mac-2/Galectin-3 immunostaining, and FACS (fluorescence-activated cell sorting) analysis ($CD45^+CD11b^+Ly6G^-CD64^+F4/80^+$cells). In contrast to macrophages, cardiac $Ly6C^{high}$ and $Ly6C^{low}$ monocytes were unaffected post-I/R compared with control mice. Mechanistically, inhibition of HA synthesis led to increased macrophage apoptosis in vivo and in vitro. In addition, α-SMA (α-smooth muscle actin)–positive cells were reduced in the infarcted myocardium and in the border zone. In vitro, the myofibroblast response as measured by *Acta2* mRNA expression was reduced by inhibition of HA synthesis and of CD44 signaling. Furthermore, *Has2* KO fibroblasts were less able to contract collagen gels in vitro. The effects of HA/CD44 on fibroblasts and macrophages post-I/R might also affect intercellular cross talk because cardiac fibroblasts were activated by monocyte/macrophages and, in turn, protected macrophages from apoptosis.**

Conclusions: **Increased HA synthesis contributes to postinfarct healing by supporting macrophage survival and by promoting the myofibroblast response. Additionally, imaging of cardiac HA by chemical exchange saturation transfer post-I/R might have translational value. (*Circ Res*. 2019;124:1433-1447. DOI: 10.1161/CIRCRESAHA.118.313285.)**

Key Words: extracellular matrix ■ hyaluronic acid ■ macrophages ■ myocardial infarction ■ reperfusion injury

In the Western countries, the mortality from acute myocardial infarction (AMI) has decreased continuously[1] during the last decades. In particular, the incidence of ST-segment–elevation myocardial infarction (STEMI) decreased in the developed countries because of the effective primary and secondary prevention strategies and the treatment of risk factors/comorbidities.[2] However, globally, the incidence of both STEMI and non-STEMI is increasing, and severe complications, such as heart failure and cardiac arrhythmia, develop in survivors of myocardial infarction. Therefore, mechanisms that could be targeted in the acute phase after AMI or myocardial ischemia/reperfusion (I/R) to improve the long-term perspective of STEMI and non-STEMI patients especially with respect to heart failure and sudden cardiac death are of great clinical interest.[3,4]

Meet the First Author, see p 1402

Received April 25, 2018; revision received March 13, 2019; accepted March 26, 2019.

From the Institut für Pharmakologie und Klinische Pharmakologie (A.P., M.G., D.J.G., M.A., M.P., R.S., S.H., J.M., S.G., J.W.F.), CARID, Cardiovascular Research Institute Düsseldorf (A.P., M.G., D.J.G., M.A., M.P., R.S., S.H., J.M., S.G., M. Kelm, A.G., U.F., J.W.F.), Institut für Molekulare Kardiologie (Z.D., U.F.), Klinik für Kardiologie, Pneumologie und Angiologie (M. Kelm, U.F.), and Institut für Herz- und Kreislaufphysiologie (S.K., M. Krüger, A.H., A.G.), University Hospital, Heinrich-Heine-University Düsseldorf, Germany; Institute of Clinical Biochemistry and Pathobiochemistry, German Diabetes Center at the Heinrich-Heine-University Duesseldorf, Leibniz Center for Diabetes Research, Germany (S.H., S.L.); German Center for Diabetes Research, München-Neuherberg, Germany (S.H., S.L.); Sanford Burnham Prebys Medical Discovery Institute, La Jolla, CA (Y.Y.); and Matrix Biology Program, Benaroya Research Institute at Virginia Mason, Seattle, WA (T.N.W.).

*A.P. and M.G. equally contributed to this article.

The online-only Data Supplement is available with this article at https://www.ahajournals.org/doi/suppl/10.1161/CIRCRESAHA.118.313285.

Correspondence to Jens W. Fischer, Institut für Pharmakologie und Klinische Pharmakologie, Universitätsklinikum der Heinrich-Heine-Universität Düsseldorf, Moorenstraße 5, 40225 Düsseldorf, Germany. Email jens.fischer@uni-duesseldorf.de

Novelty and Significance

What Is Known?

- Cardiac ECM (extracellular matrix) remodeling stabilizes the infarct scar and is important for adaptation to ischemia and reperfusion (I/R) injury. However, continued remodeling leading to interstitial fibrosis impairs contractile function.
- The functional interactions of fibroblasts and immune cells and their activation are pivotal for a balanced healing response after cardiac I/R.
- Hyaluronan—a carbohydrate of the ECM—is rapidly synthesized de novo in models of wounding and inflammation.

What New Information Does This Article Contribute?

- After myocardial I/R, hyaluronan (HA) is rapidly synthesized by HAS (HA synthase) 2 and accumulates within the first 24 h in the infarcted left ventricle.
- Myocardial HA accumulation can be visualized in vivo by magnetic resonance imaging using chemical exchange saturation transfer.
- Deletion of *Has2* causes increased apoptosis in cardiac macrophages and decreased cardiac fibroblasts activation involving reduced TGF (transforming growth factor)-β signaling.

Cell-mediated HA synthesis by HAS2 is an acute response to cardiac ischemia and can be visualized and quantified by cardiac chemical exchange saturation transfer magnetic resonance imaging. Deletion of *Has2* results in ventricular dilatation, increased scar size, and decreased ejection fraction, suggesting that cardiac HA is crucial for infarct healing. We show here that the myocardial HA matrix is indispensable for proper macrophage and fibroblast responses. Specifically, apoptosis of monocyte-derived and resident macrophages was increased in the absence of HAS2. At the same time, the activation and function of cardiac fibroblasts was inhibited by reduced HA/CD44 signaling. Based on the rapid onset of HA synthesis after I/R and its functional importance for hemodynamic adaptation, these results suggest that HA may be a promising prognostic marker or therapeutic target in the acute phase post-I/R.

Nonstandard Abbreviations and Acronyms

α-SMA	α-smooth muscle actin
4-MU	4-methylumbelliferone
AKT	serine/threonine protein kinase
AMI	acute myocardial infarction
CD	cluster of differentiation
CEST	chemical exchange saturation transfer
ECM	extracellular matrix
ERK	extracellular signal–regulated kinase
FACS	fluorescence-activated cell sorting
HA	hyaluronan
HAS	hyaluronan synthase
I/R	ischemia/reperfusion
IL	interleukin
LV	left ventricle
MHC	major histocompatibility complex
MMP	matrix metalloproteinase
PI3K	phosphoinositide 3-kinase
RHAMM	receptor of HA-mediated motility
SMAD	mothers against decapentaplegic homolog
STEMI	ST-segment–elevation myocardial infarction
TGF	transforming growth factor

The ECM (extracellular matrix) provides a 3-dimensional scaffold to the heart that facilitates force transduction and maintenance of cellular architecture. Further, ECM forms a stable microenvironment facilitating the function of both cardiomyocytes and noncardiomyocytes.[5] On ischemic injury and cardiomyocyte death, the ECM is acutely damaged by, for example, reactive oxygen species and activation of MMPs (matrix metalloproteinases). Subsequently, remodeling of the ECM is initiated involving de novo synthesis of ECM components not present in the healthy heart.[5] Cardiac ECM remodeling, especially de novo formation and cross-linking of the collagenous matrix, stabilizes the infarct scar and is important for adaptation.[6] However, continued remodeling that leads to interstitial fibrosis impairs contractile function and contributes to diastolic dysfunction.[7]

Instead of targeting the collagenous remodeling that occurs chronically after I/R, it is attractive to define mechanisms that are activated early after cardiac ischemia and set the stage for the chronic adverse remodeling. Among these mechanisms, the inflammatory response has been analyzed in great detail.[8] Myocardial ischemia leads to cardiomyocyte death and endothelial leakage initiating an intense immune cell infiltration that aims to remove cellular debris and damaged ECM. Almost all immune cells of the innate and adaptive immune response are involved in this sterile inflammation, and monocyte/macrophages are thought to be the most important effector cells for infarct healing.[9] This acute inflammatory phase is followed by a reparative, proliferative phase that involves both immune cells (reparative macrophages) and the activation of fibroblasts and angiogenic responses. However, our understanding of the fibroblast response is far from complete.[5,10] Similarly, the role of the complex noncollagenous matrix[11] that is synthesized de novo early after infarct is incompletely understood. However, this early provisional ECM likely is—in conjunction with growth factors, cytokines, and chemokines—critical for the phenotypes of immune cells, cardiac fibroblasts, pericytes, and endothelial cells in the acute phase after cardiac ischemia.

An interesting candidate ECM system in this regard is hyaluronan (HA). HA is a carbohydrate formed from repeating disaccharides (D-glucuronic acid and *N*-acetyl-D-glucosamine) linked by a glucuronidic β(1→3) bond. HA is synthesized by HAS (HA synthases) 1–3 at the plasma membrane and associates with different HA-binding proteins to form pericellular and extracellular HA matrix networks. Furthermore, HA signals through CD (cluster of differentiation) 44 and RHAMM (receptor of HA-mediated motility). From other pathologies such as neointimal hyperplasia,[12] atherosclerosis,[13] and autoimmune[14] diseases, it has been recognized that HA strongly affects

immune responses.[15] Additionally, HA drives volume expansion and activation of fibroblasts during disease-associated remodeling and embryonic development.[16,17] These roles of HA are, in part, mediated by HA receptors RHAMM and CD44 and, in part, by the fact that HA provides a very loose permissive matrix that facilitates cell movements. The abovementioned functions of HA contribute to wound healing and on the contrary in cardiovascular diseases also promote pathological hyperplastic responses including intimal hyperplasia during atherosclerosis.[15,18]

In the adult heart, HA accumulates strongly in the perivascular matrix, but only very small amounts are present in the interstitial matrix of the myocardium. Interestingly, cardiac HA synthesis by HAS2 is critically required for cardiac development during embryogenesis. Specifically, chamber septation and heart valve formation are disturbed in *Has2*$^{-/-}$ mice causing embryonic lethality.[19] Deletion of the other 2 *Has* genes, *Has1* and *Has3*, did not lead to a cardiac phenotype. Although we and others reported the accumulation of HA post-myocardial infarction, the function of HA post-myocardial infarction is yet unknown.[20,21]

In the current study, we aimed to investigate the role of the early cardiac HA matrix after I/R injury of the heart. Furthermore, we attempted to develop a magnetic resonance imaging (MRI) approach for cardiac HA matrix to monitor HA accumulation in vivo and to provide a translational perspective for future studies.

Methods

The data that support the findings of this study are available from the corresponding author on reasonable request. A detailed description is provided in the Online Data Supplement.

Mice

Male 12- to 18-week-old C57BL/6J mice (Janvier Labs, Le Genest-Saint-Ile, France), Rosa26CreER$^{T2+/-}$ mice (Taconic, Hudson, NY[22]), and Rosa26CreER$^{T2+/-}$;Has2$^{flox/flox}$ mice,[23] as well as *Has1*$^{-/-}$ mice[24] and respective littermate controls, all on a C57BL/6J background, were used for experiments. Rosa26CreER$^{T2+/-}$ mice and Rosa26CreER$^{T2+/-}$;Has2$^{flox/flox}$ mice were treated intraperitoneally for 5 days with 1 mg per mouse per day tamoxifen (Sigma, Darmstadt, Germany) 3 weeks before induction of myocardial I/R injury. All mice underwent myocardial I/R injury as described previously.[25,26] All mice with a sufficient knockdown of *Has2* that received a successful I/R injury as determined by visualization of ST-segment elevation and displayed no signs of infection after surgery were included in the analyses. Mice were excluded from the experiment when certain criteria of suffering were observed. These included weight loss >20% of body weight, cessation of food and water ingestion, or lack of voluntary movement.

Permission for animal experiments was granted by the Landesamt für Natur, Umwelt und Verbraucherschutz Nordrhein-Westfalen, Bezirksregierung Düsseldorf, Aktenzeichen 84-02.04.2012.A138 and Aktenzeichen 84-02.04.2015.A322.

Magnetic Resonance Imaging

Data were recorded at a Bruker AVANCE^{III} 9.4T wide bore NMR (nuclear magnetic resonance) spectrometer driven by ParaVision 5.1 (Bruker, Rheinstetten, Germany) and operating at frequencies of 400.21 MHz for ^{1}H and 376.54 MHz for ^{19}F measurements. Images were acquired using a Bruker microimaging unit Micro 2.5 with actively shielded gradient sets (1.5 T/m) and a 25-mm birdcage resonator tunable to both ^{1}H and ^{19}F as described previously.[27,28] Mice were anaesthetized with 1.5% isoflurane and kept at 37°C. The front paws and the left hind paw were attached to ECG electrodes (Klear-Trace; CAS Medical Systems, Branford), and respiration was monitored by means of a pneumatic pillow positioned at the animal's back. Vital functions were acquired by a M1025 system (SA Instruments, Stony Brook, NY) and used to synchronize data acquisition with cardiac and respiratory motion.

For functional analysis, high-resolution images of mouse hearts were acquired in short-axis orientation using an ECG- and respiratory-gated segmented cine fast gradient echo cine sequence with steady-state precession essentially as described before.[29] A flip angle of 15°, echo time of 1.2 ms, and a repetition time of about 6 to 8 ms (depending on the heart rate) were used to acquire 16 frames per heart cycle. The pixel size after zero filling was 117×117 μm^2 (field of view, 30×30 mm^2; acquisition time per slice for 1 cine sequence, ≈1 minute). Eight to 10 contiguous slices were acquired to cover the entire heart. Routinely, 8 to 10 short-axis slices were required for complete coverage of the left ventricle (LV). For evaluation of functional parameters (eg, end-diastolic volume, end-systolic volume, and ejection fraction), ventricular demarcations in end diastole and end systole were manually drawn with the ParaVision region-of-interest tool (Bruker, Rheinstetten, Germany). For late gadolinium enhancement, a bolus of Gd-DTPA (gadolinium-diethylenetriaminepentacetate; 0.2 mmol Gd-DTPA per kg body weight) was applied intraperitonally.

Results

Interference With Cardiac HA Matrix Formation Post-I/R Severely Impairs Hemodynamic Function

HA has been attributed important roles in proliferation of various cell types in wound healing[16] and in inflammation.[15] From morphological analyses in canine and murine infarcts,[20] it is known that HA affinity staining increases after I/R at 14 days in dogs and after 3 and 7 days in mice. Here, we demonstrate an even earlier induction of *Has1* and *Has2* mRNA in the murine I/R model at 6 hours post-I/R (Online Figure I) suggesting an acute onset of cardiac HA synthesis after I/R. Considering the rapid onset of *Has1* and *Has2* expression and the known functions of HA in other tissues and diseases, we tested the hypothesis that cardiac HA synthesis after I/R injury represents an endogenous repair mechanism.

To analyze the function of de novo HA synthesis after I/R, we utilized mice deficient for the 2 enzymes that were induced after I/R, *Has2* and *Has1*, to determine the involvement of endogenous HA synthesis in an experimental model of I/R. Whereas *Has1* deletion is constitutive, *Has2* deletion was induced by application of tamoxifen in adult mice as described in the Online Data Supplement because of embryonic lethality of constitutive *Has2* KOs (*Has2* deficient).[19] In addition, mice were treated with the pharmacological inhibitor of HA synthesis, 4-methylumbelliferone (4-MU).

Inhibition of HA synthesis by deletion of *Has2* (Figure 1) and by 4-MU (Online Figure IIA) did not affect the initial ischemic area as determined by late gadolinium enhancement. Importantly, in the long-term follow-up deletion of *Has2* (Figure 1B) and 4-MU treatment (Online Figure IIB) severely impaired hemodynamic function as indicated by decreased ejection fractions determined by MRI. However, whereas *Has2* deletion was characterized by strongly increased end-systolic and end-diastolic volumes (Online Table III), 4-MU treated mice developed no changes end-systolic volume and end-diastolic volume but instead showed strongly decreased stroke volume and cardiac output. This difference to *Has2* KO mice and the known off target effects of 4-MU such as biosynthesis inhibition of other polysaccharides containing D-glucuronic acid, the inhibition of MMPs, and metabolic effects in vivo led us to focus only on the genetic deletion of *Has* isoforms for mechanistic experiments in vivo. 4-MU was considered as additional proof of concept for the development of the chemical exchange

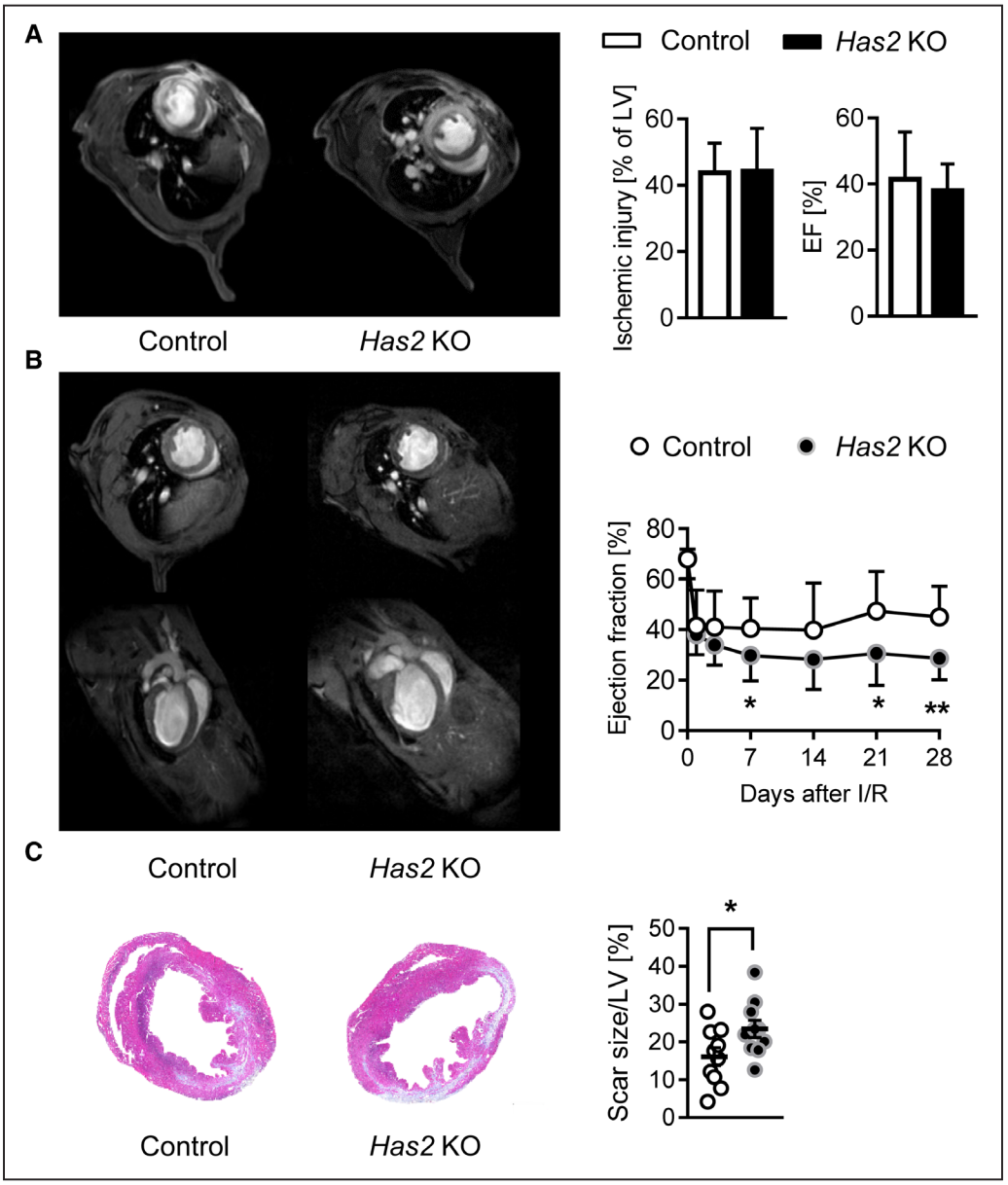

Figure 1. Deletion of *Has2* impairs cardiac function post-ischemia and reperfusion (I/R) injury. *Has2* KO (*Has2* deficient) and control mice were subjected to I/R injury; hemodynamic function and infarct size were analyzed by magnetic resonance imaging (MRI) and histology. **A**, Late gadolinium enhancement was used to determine ischemic injury and cine loops for ejection fraction 24 h post-I/R, n=9, 9. **B**, Cardiac function determined by MRI at baseline, 1, 3, 7, 14, 21, and 28 d post-I/R injury, n=9, 9. **C**, Scar size as determined by Gomori trichrome staining 3 wk post-I/R, n=10, 10. Data represent mean±SD (**A** and **B**) and mean±SEM (**C**). LV indicates left ventricle. **P*<0.05, ***P*<0.01.

saturation transfer (CEST) MRI (see below, Figure 2) in parallel with *Has2*- and *Has1*-deficient mice.

To focus on the long-term effects of *Has2* deletion, the scar size was analyzed 3 weeks after I/R and was found to be increased in *Has2* KO mice (Figure 1C). In contrast, deletion of *Has1* had no significant effect on cardiac function and scar size (Online Figure III). Tension-to-rupture experiments were performed in LV stripes 3 weeks days after I/R to evaluate whether the stability of the scar tissue was affected as shown before in mice deficient in collagen modifying proteoglycans.[30] This analysis revealed only a trend toward reduced scar stability in *Has2* KO hearts (Online Figure IV) and thereby excludes major changes in the collagenous matrix in the chronic phase after I/R. Next, effects of HA on angiogenesis were considered. Twenty-one days after I/R, angiogenic responses in the remote and borderzone of *Has2* KO mice were unaffected (Online Figure V).

These data clearly indicate that endogenous HA synthesis post-I/R especially by HAS2 is an immediate, protective response that does not acutely affect infarct size but is instead required in the subacute phase post-I/R. This was confirmed in Langendorff experiments that revealed no acute functional differences after I/R between control and *Has2* KO hearts (Online Figure VI) ex vivo.

HA Accumulates Early After I/R Injury and Can Be Imaged by CEST

To characterize the endogenous HA response in the ischemic hearts in more detail, we attempted to adjust MRI CEST

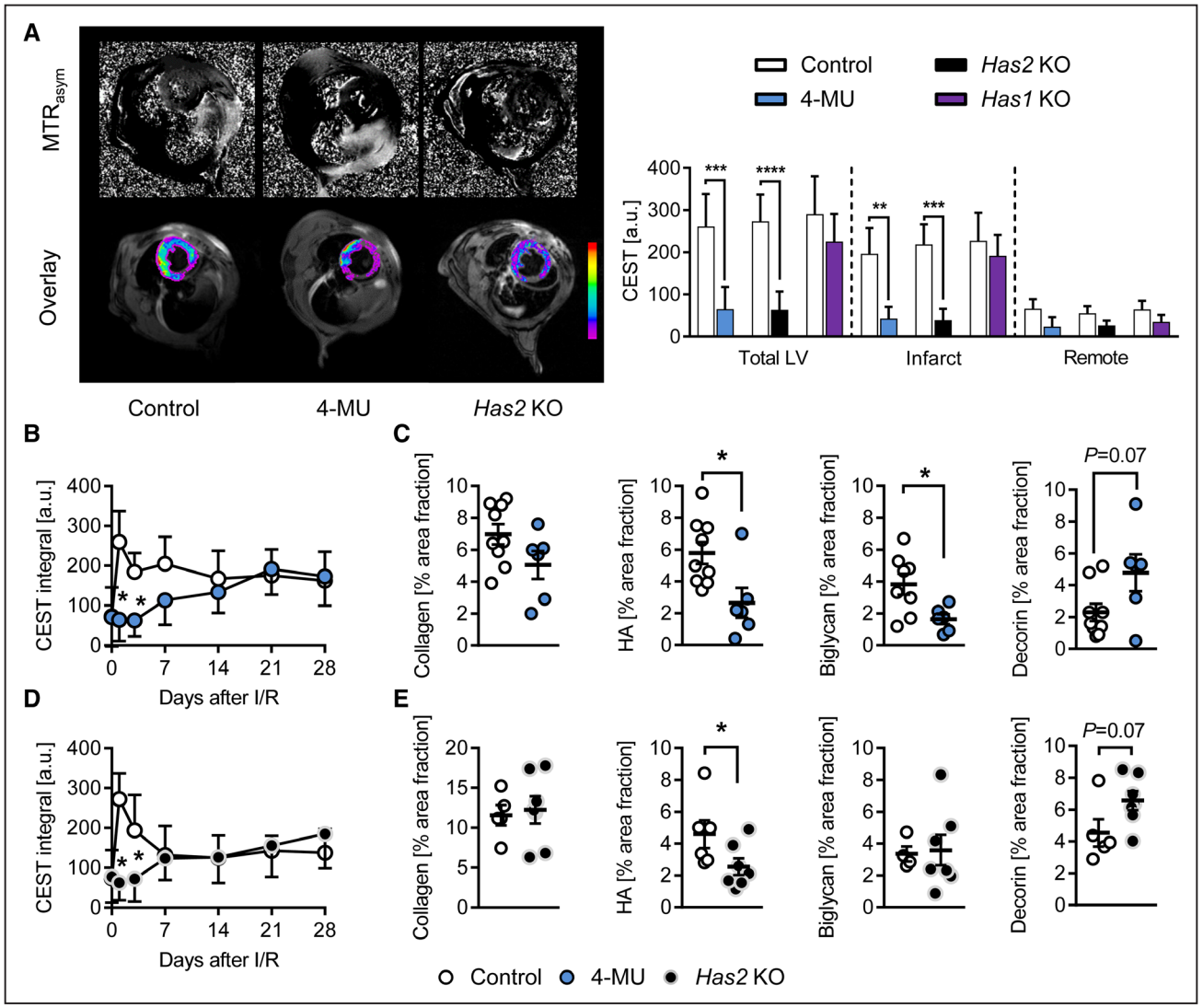

Figure 2. Magnetic resonance imaging (MRI) of decreased cardiac hyaluronan (HA) accumulation post-ischemia and reperfusion (I/R) in 4-methylumbelliferone (4-MU)–treated mice and *Has2* KO (*Has* deficient) mice. A, Representative cardiac chemical exchange saturation transfer (CEST) MRI images (**left**) and quantification of cardiac CEST signal 24 h post-I/R (**right**) in total left ventricle (LV), infarct, and remote regions of 4-MU–treated, *Has2* KO, and *Has1* KO mice and their respective controls; mean±SD, n=4. Time course of cardiac CEST signal and respective quantification of collagen staining, HA affinity histochemistry, biglycan and decorin immunostaining in 4-MU–treated mice (**B** and **C**) and *Has2* KO mice (**D** and **E**). Mean±SD, n=4 (**B** and **D**) and mean±SEM, n=6 to 9 (**C**) and n=5 to 7 (**E**). MTR_{asym} indicates magnetization transfer ratio asymmetry. **P*<0.05, ***P*<0.01, ****P*<0.001, *****P*<0.0001.

techniques[31,32] to monitor cardiac matrix accumulation including HA after I/R injury as a function of time after injury. Although the CEST signal is not specific for a certain matrix component, the amount of exchangeable protons is especially high in hydroxylated sugar moieties of HA and glycosaminoglycans. As shown in Online Figure VIIA, HA gives rise to the strongest CEST signal followed by proteoglycans and heparin, whereas collagen (gelatin and fibrillar collagen), hydroxyproline, and matrigel result in much weaker signals in z-spectra acquired from individual phantoms. Similar z-spectra were obtained from the LV 24 hours after I/R in mice (Online Figure VIIB and VIIC). With respect to the location of HA, strong CEST signals were detected in the infarcted LV with lower intensity in the border zone and almost no signal in the remote myocardium (Online Figure VIIC) 24 hours post-I/R injury. To further enhance specificity and to avoid potential contaminations from CEST-active components in the blood (in particular sugars and glycosylated compounds), before induction of saturation, a black blood preparation was initiated for suppression of all signals from circulating blood (see the Online Data Supplement for more details, Online Figure VIII). In line with the CEST signal, affinity histochemistry detected HA accumulation already 24 hours post-I/R (Online Figure IX). In contrast, the staining of other ECM molecules associated with collagen scar formation revealed that these did not accumulate.[20] Specifically, collagen stained by Picrosirius Red and immunostaining of 2 collagen-binding proteoglycans that are known to be upregulated post-AMI (decorin and biglycan) showed no positive signal 24 hours post-I/R (Online Figure IX). This is in line with upregulation of these matrix compounds simultaneously or subsequently to fibroblast activation,[20,30] which is initiated around 3 days post-I/R. Together, these data show that cardiac HA accumulation occurs within 24 to 48 hours post-I/R and is detectable by CEST in vivo.

After establishment of the cardiac CEST MRI, the CEST approach was used (1) to monitor cardiac HA over time and under different experimental conditions and (2) to investigate mice treated with the pharmacological inhibitor of HA synthesis, 4-MU, and mice deficient of *Has2* and *Has1*. As shown in Figure 2A, both 4-MU and *Has2* KO led to a strongly reduced CEST signal 24 hours after I/R injury. The reduction in HA was more pronounced in the infarct region compared with the remote zone. In contrast, only a small decrease by trend occurred in *Has1* KOs. Subsequently, the temporal development of the CEST signal was compared with the time course of morphological analysis of HA, collagen, biglycan, and decorin (Figure 2B through 2E). In the respective control groups, the CEST signal increases about 3-fold within 24 hours post-I/R (Figure 2B and 2D). Both 4-MU treatment and *Has2* deficiency caused a strong reduction of cardiac CEST signals during the first 3 days post-AMI (Figure 2B and 2D). These data clearly indicate that cardiac CEST MRI allows to monitor HA accumulation post-I/R, especially in the first 1 to 3 days post-I/R. Interestingly, after 7 and 14 days, the CEST signals in 4-MU and *Has2* KO mice approached those of controls most likely representing the increasing accumulation of the other ECM components such as proteoglycans, cellular fibronectin, thrombospondin, and subsequently, collagens. As mentioned above, the lack of diminished CEST signal in *Has1* KO mice after I/R (Figure 2A) suggested that HAS1-derived HA is quantitatively less compared with the HAS2-derived HA. In line with this assumption is the finding that the hemodynamic function was not affected in *Has1* KOs in contrast to *Has2* KO and 4-MU–treated mice (Online Figure III; Online Table III).

HAS2 Is Required for Myofibroblast Responses

Next, it was considered that *Has2* deletion affects either the fibroblast response or the inflammatory response post-I/R. First, fluorescent stainings of HA/α-SMA (α-smooth muscle actin) and HA/Mac-2 were performed in the infarct zone revealing that both cell types are in close contact with the cardiac HA matrix (Figure 3A and 3B). Isolated cardiac fibroblasts released substantial amounts of HA basally and in response to TGF (transforming growth factor)-β1 in vitro (Figure 3C). Of note, although about 10× less, monocytes isolated from the bone marrow released HA as well, and even bone marrow–derived macrophages secreted small amounts of HA. The main isoenzyme within fibroblasts was HAS2 (Figure 3D).The fibroblast/myofibroblast response was analyzed by immunostaining of vimentin that labels all cardiac cells with the exception of cardiac myocytes and α-SMA indicating myofibroblast activation (Figure 4A and 4B). Whereas vimentin was not affected, the amount of α-SMA–positive cells was decreased in *Has2* KO versus control mice. Further analysis revealed that α-SMA–positive cells were reduced by trend in the infarct zone and significantly in the border zone but not in the remote myocardium (Figure 4C through 4E). The proliferation of myofibroblasts at 72 hours after I/R injury trended toward reduction in *Has2* KO hearts as indicated by Ki67/α-SMA double stainings (Figure 4C and 4D). TGF-β1 is induced early after I/R and is an important growth factor for myofibroblast activation and reparative remodeling of ECM, as well as a modulator of the transition between the inflammatory phases after I/R.[33] To address possible changes in canonical and noncanonical TGF-β signaling, cardiac LV lysates were analyzed 72 hours after I/R with respect to phosphorylation of SMAD2 (mothers against decapentaplegic homolog), ERK (extracellular signal–regulated kinases) 1/2, and an AKT (serine/threonine protein kinase; Online Figure X) by immunoblotting. Interestingly, inhibition of AKT phosphorylation was evident in samples of *Has2* KO mice. Furthermore, small trends toward reduced SMAD2 and ERK1/2 phosphorylation were observed.

For further mechanistic insight, fibroblasts were isolated from *Has2* KO and control hearts and analyzed in vitro in the first passage. *Has2* KO fibroblasts were less responsive to FCS with respect to proliferation (Figure 5A) underlining the trends toward less proliferation observed in vivo 72 hours post-I/R. As expected, *Has2* expression (data not shown) and HA synthesis were reduced in *Has2* KO cells (Figure 5B). Compensatory upregulation of *Has1* and *Has3* was not observed on deletion of *Has2* (data not shown). The ability of cardiac fibroblasts to contract fibrillar collagen gels in vitro was used as a functional test of the myofibroblastic phenotype. Indeed both *Has2* deletion and 4-MU (Figure 5C) strongly reduced the ability of cardiac fibroblasts to contract collagen gels. The myofibroblastic differentiation as detected by *Acta2* mRNA expression in response to TGF-β1 was strongly reduced if HA synthesis was inhibited by 4-MU (Figure 5D) or a blocking antibody directed toward CD44's HA-binding domain (Figure 5E) was applied. To further address the role of CD44 in activation of TGF-β1 signaling, SMAD2 phosphorylation was determined. As shown in Figure 5F, blocking CD44 indeed reduced TGF-β1–induced phosphorylation of SMAD2, whereas noncanonical TGF-β responses, such as AKT and ERK phosphorylation, were not affected (data not shown).

HA/HAS2 Is Needed for Cardiac Macrophage Responses Post-I/R

The uptake of perfluorocarbon particles was used to monitor the accumulation of phagocytic immune cells (mainly macrophages[27]) post-I/R in *Has2* KO mice. In turn, $^{1}H/^{19}F$ MRI[27] revealed a strongly reduced ^{19}F signal from perfluorocarbon-labeled immune cells in the infarcted LV indicative of anti-inflammatory effects in *Has2* KO mice (Figure 6A). This was paralleled by changes in the concentration of circulating chemokines and cytokines, such as reductions of MCP-1/CCL2 (C-C chemokine receptor type 2), IL (interleukin)-13, and RANTES/CCL5 (CC-chemokine ligand 5; Online Figure XI). Subsequently, detailed flow cytometric measurements of the heart at different times post-I/R were performed. At 24 hours post-I/R, cardiac immune cells in *Has2* KO hearts (Online Figure XII) and blood (Online Figure XIII) were comparable to control mice. To exclude possible earlier effects especially on invading neutrophils, hearts were also analyzed 12 hours post-I/R. However, no differences between *Has2* KO mice and control mice were found (data not shown).

Subsequently, cardiac immune cells were investigated 72 hours post-I/R. Total cardiac monocytes ($MHCII^{low}CCR2^{+}$), neither $Ly6C^{high}$ nor $Ly6C^{low}$, were not altered in *Has2* KO hearts compared with control (Figure 6B through 6D). However, the amount of cardiac macrophages ($F4/80^{+}CD64^{+}$) and monocyte-derived macrophages ($MHCII^{high}CCR2^{+}$) was decreased

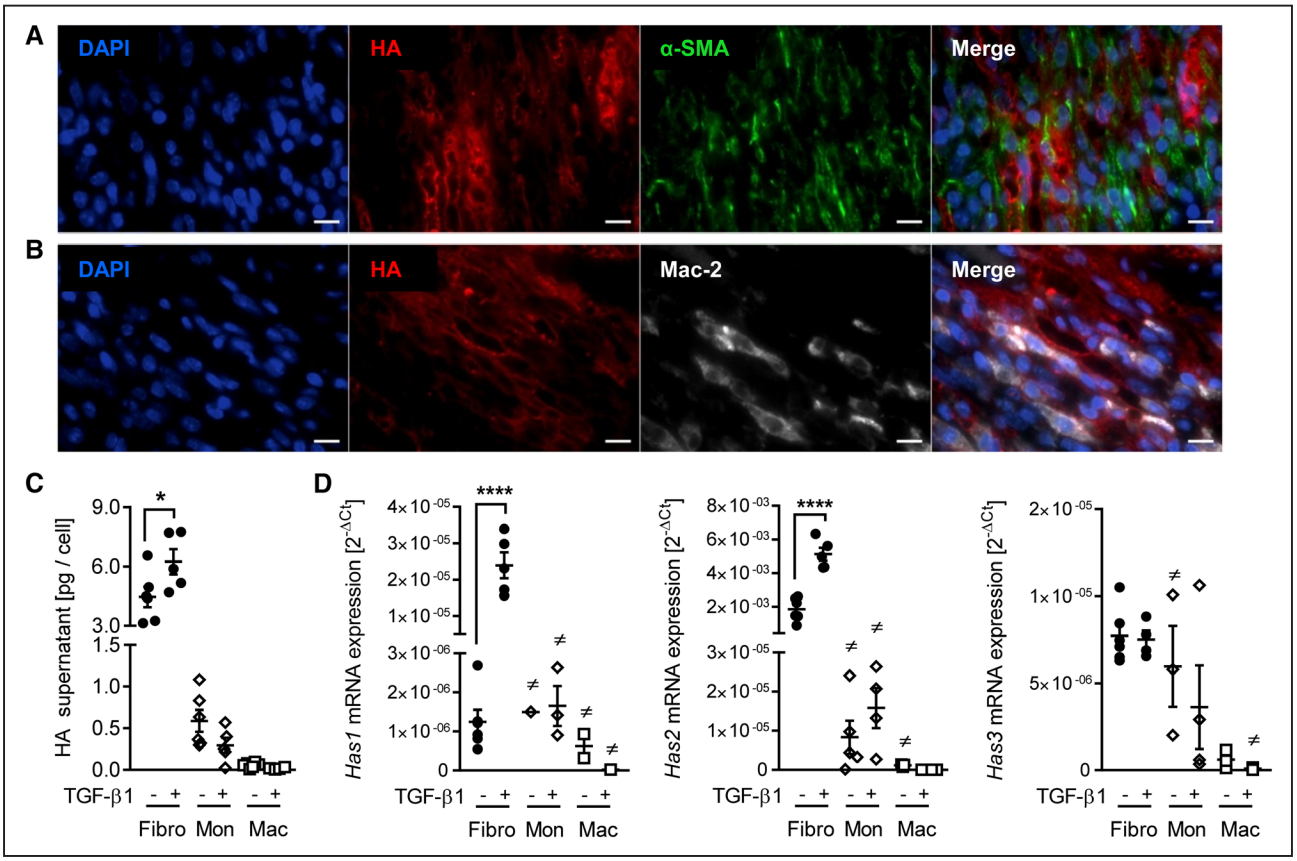

Figure 3. Hyaluronan (HA) production of cardiac fibroblasts (Fibro), monocytes (Mon), and macrophages (Mac). A, Costaining of HA/α-SMA (α-smooth muscle actin) and (**B**) HA/Mac-2 (Galectin-3) within the infarct zone 72 h post-ischemia and reperfusion. Scale bar indicates 10 µm. Cardiac Fibro, Mon, and bone marrow–derived Mac were isolated from C57BL6/J mice. **C**, HA secretion into the supernatant and (**D**) *Has 1*, *2*, and *3* mRNA expression after 24-h stimulation with (+) or without (–) TGF (transforming growth factor)-β1 (10 ng/mL). The numbers of samples with no detectable *Has* mRNA expression (≠) in each group were as follows: *Has1*; monocytes –TGF-β1: 5 from 6 samples, +TGF-β1: 2 of 5, Mac –TGF-β1: 4 of 6, +TGF-β1: 4 of 5. *Has2*; monocytes –TGF-β1: 1 of 6, +TGF-β1: 1 of 5, Mac –TGF-β1: 3 of 6. *Has3*; monocytes –TGF-β1: 2 of 6, Mac –TGF-β1: 3 of 6. Data represent mean±SEM, n=5 to 6; **P*<0.05, *****P*<0.0001. DAPI indicates 4′,6-diamidino-2-phenylindole.

(Figure 6E and 6F). Resident MHCII^{high} CCR2^{-} macrophages were also reduced in *Has2* KO mice in contrast to MHCII^{low}CCR2^{-} macrophages (Figure 6G). A representative gating scheme is depicted in Online Figure XIV. Cardiac lymphocyte subsets were not affected (Online Figure XV). In addition, circulating immune cells (Online Figure XVI), splenic immune cells (Online Figure XVII), and immune cells in the bone marrow (Online Figure XVIII) were unaffected 72 hours after I/R.

Our data indicate that monocyte recruitment to the ischemic heart was not disturbed (as indicated by comparable numbers of systemic and local invading monocytes). Furthermore, we detected no differences between *Has2* KO and control mice in mRNA expression of chemokines, cytokines, and cytokine receptors 72 hours post-I/R as determined by a polymerase chain reaction array from infarcted LV samples (Online Table V). This suggested that the expression of inflammatory genes by the majority of cardiac cell is, at least in average, unchanged. Instead, our FACS (fluorescence-activated cell sorting) data (Figure 6) suggest very specific effects on monocyte-derived macrophages and resident macrophages. Mechanistically, either effects on monocyte to macrophage differentiation, macrophage proliferation, or an increase in macrophage apoptosis were considered. Differences in macrophage proliferation were ruled out by Ki67/Mac-2 costaining in the total LV (Figure 7A), as well as in infarct, border, and remote zone (Online Figure XIX). Unchanged proliferation was confirmed by flow cytometric enumeration of BrdU (5-bromo-2'-deoxyuridine)-positive monocytes (Figure 7B), total BrdU^{+} macrophages (Figure 7C), and BrdU^{+} monocyte-derived macrophages (Figure 7D) in the infarcted heart. When investigating monocyte-to-macrophage transition in vitro, we observed no differences between monocytes isolated from control mice and *Has2* KO mice in response to M-CSF (macrophage colony-stimulating factor; Online Figure XX). Importantly, we detected more apoptotic macrophages (Figure 7E and 7F) in hearts from *Has2* KO mice compared with control mice 72 hours post-I/R. In line, increased apoptosis was also detected in cultures of bone marrow–derived macrophages in conditions with reduced HA synthesis or CD44 signaling thereby pointing toward antiapoptotic HA-mediated effects on macrophages (Online Figure XXIA and XXIB). Using a blocking antibody for the HA-binding domain of CD44 (Online Figure XXIC), these in vitro experiments suggested that effects on macrophage apoptosis are dependent on HA/CD44 signaling. Interestingly, no effects on apoptosis were observed when investigating annexin V binding in MEFSK4^{+} fibroblasts by flow cytometry 72 hours post-I/R (Online Figure XXII). Finally, the secretome of bone marrow–derived macrophages of *Has2* KO mice was analyzed (Online Figure XXIII). These

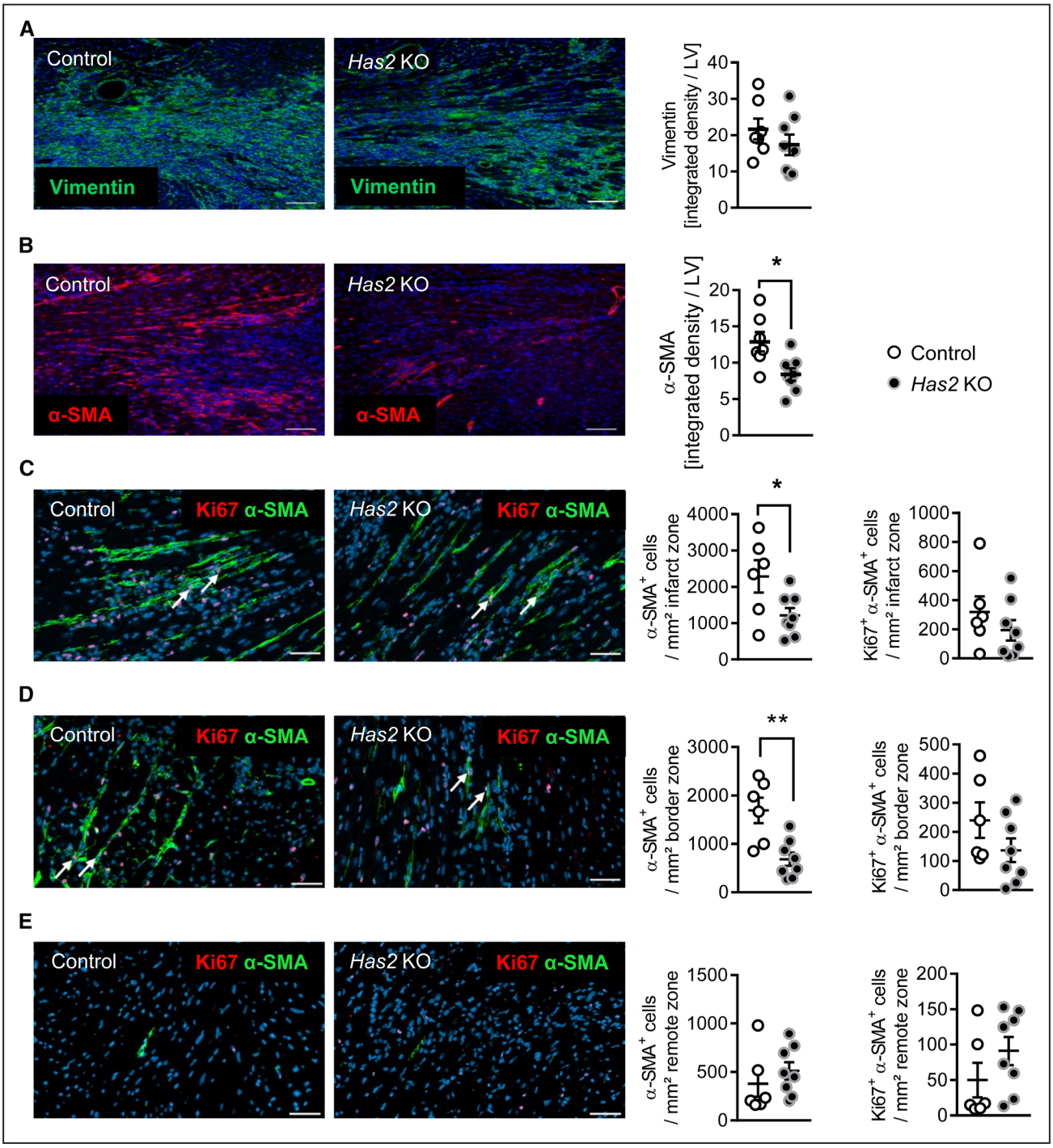

Figure 4. Reduced myofibroblast response in *Has2* KO (*Has* deficient) mice. Hearts of *Has2* KO and control mice were harvested 72 h after ischemia and reperfusion injury. **A**, Staining of heart sections for vimentin (**left**) and respective quantification per left ventricle (LV; **right**), n=7, 8. **B**, Staining of heart sections for α-SMA (α-smooth muscle actin; **left**) and respective quantification per LV (**right**), n=7, 8. **C**–**E**, Staining of heart sections for Ki67 and α-SMA (**left**) and respective quantification (**right**) of α-SMA–positive and Ki67/α-SMA double-positive cells in (**C**) infarct zone, (**D**) borderzone, and (**E**) remote zone, n=6, 8. Arrows indicate Ki67/α-SMA double-positive cells. Data represent mean±SEM; **P*<0.05; ***P*<0.01. Scale bar=100 μm in **A** and **B**; 50 μm in **C**–**E**.

data indicate reduced secretion of cytokines such as CCL2 and CXCL1 (chemokine (C-X-C motif) ligand 1).

Has2 Deficiency Impairs Instructive Interactions of Monocyte/Macrophages and Fibroblasts

Finally, the interrelationship between fibroblasts and monocytes/macrophages was investigated. Coculture experiments showed a strong effect of monocytes on fibroblast activation and promotion of a myofibroblast phenotype as shown by α-SMA staining (Online Figure XXIVA) and increased *Acta2* mRNA expression (Online Figure XXIVB). Importantly, cell activation was also detected vice versa in monocytes when cultured in the presence of fibroblasts: As shown in Online Figure XXIVC, transition from monocytes to macrophages

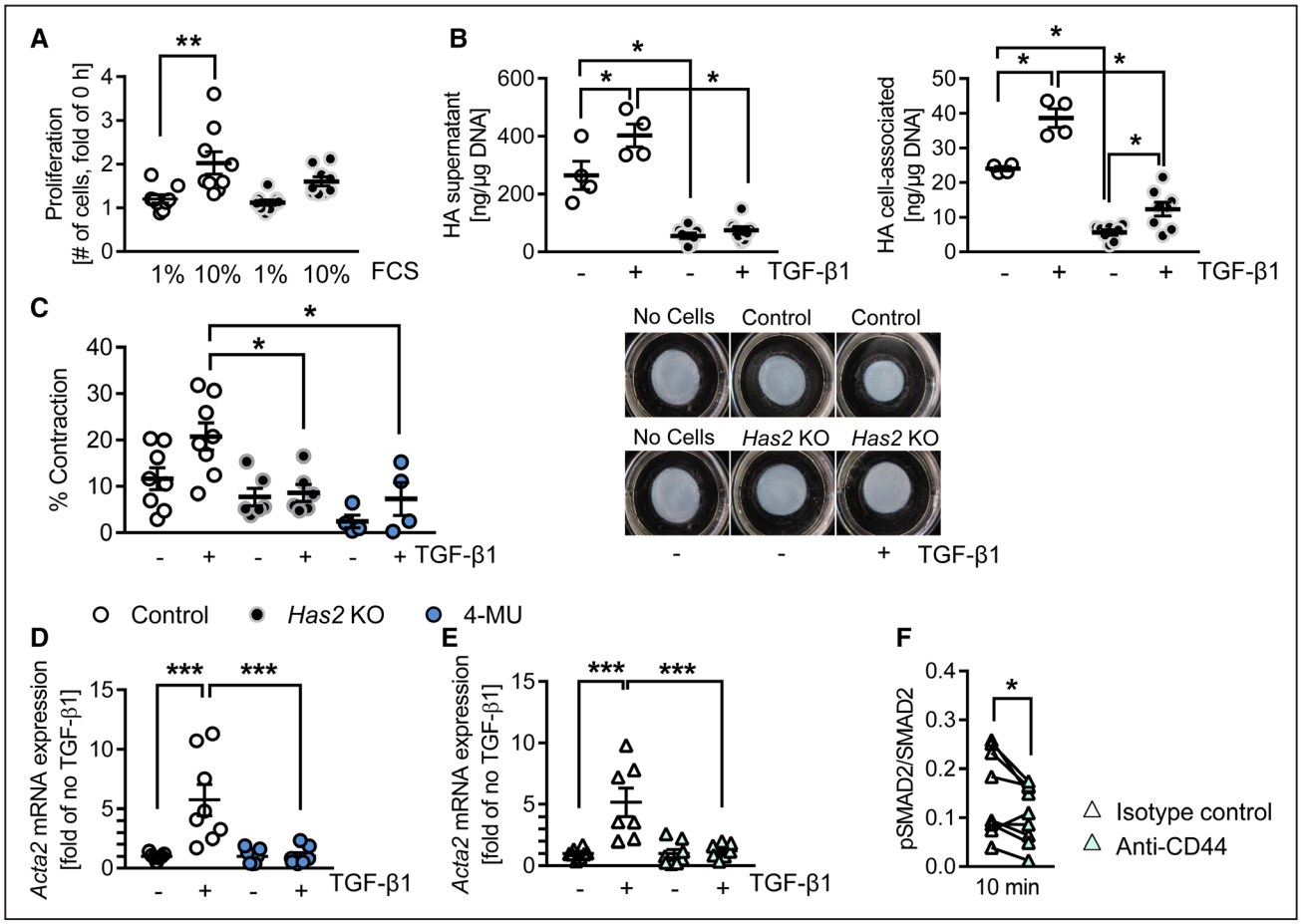

Figure 5. TGF (transforming growth factor)-β1–driven cardiac fibroblast activation is inhibited by 4-methylumbelliferone (4-MU) and blocking CD44/hyaluronan (HA) interaction. A, Proliferation in response to FCS was determined in *Has2* KO (*Has2* deficient) and control cells; n=9. **B**, HA was determined in the supernatant and the cell layer revealing reduced HA in *Has2* KO cells, n=4, 4, 8, 8. **C**, Contraction of collagen gels by cardiac fibroblasts with knockout of *Has2* and those treated with 4-MU was inhibited, n=8 (control), n=6 (*Has2* KO), n=4 (4-MU). Cardiac fibroblasts were isolated, and the mRNA expression of *Acta2* was determined 48 h after stimulation with (+) or without (–) TGF-β1 (10 ng/mL) in the presence of (**D**) 4-MU (100 µmol/L) or respective control, n=7, 8, 7, 7 and (**E**) anti-CD44 blocking antibody (KM201; 10 µg/mL) or respective isotype control ($IgG_1\kappa$, 10 µg/mL), n=8, 7, 8, 7. **F**, pSMAD2/SMAD2 ratio was determined by Western blotting in response to TGF-β1 (10 ng/mL, 10 min) in cells pretreated for 1 h with anti-CD44 blocking antibody (KM201, 10 µg/mL) or respective isotype control ($IgG_1\kappa$, 10 µg/mL), n=9, 9. Data represent mean±SEM; **P*<0.05, ***P*<0.01, *****P*<0.001. CD indicates cluster of differentiation; pSMAD2, phosphorylated mothers against decapentaplegic homolog 2; and SMAD2, mothers against decapentaplegic homolog 2.

was increased in the presence of fibroblasts to a similar extent as in the presence of M-CSF. Further, coculture of monocytes with fibroblasts protected from macrophage apoptosis (Online Figure XXIVD). However, this effect was independent of *Has2* expression in fibroblasts.

In summary, the data obtained in *Has2* KO mice suggest that decreased cardiac HA synthesis immediately post-I/R causes both impaired fibroblast to myofibroblast differentiation, as well as an increase in macrophage apoptosis, ultimately leading to impaired healing post-I/R. The main findings of the current investigations are summarized in Figure 8.

Discussion

The current results clearly show that murine hearts react strongly with increased HA synthesis and HA deposition to I/R injury. It is shown that inhibition of this HA response by genetic deletion of *Has2* aggravates the hemodynamic dysfunction and increases scar size. Importantly, the HA-rich microenvironment critically affects 2 major cell types that ensure proper infarct healing: macrophages and cardiac fibroblasts. Thereby, the early HA response appears to be part of critical endogenous repair mechanisms after I/R.

The adult mouse myocardium contains large quantities of cardiac fibroblasts that maintain the cardiac ECM. On I/R, fibroblasts become activated and develop a secretory and proliferative phenotype. The concomitant release of fibroblast-derived cytokines and growth factors, as well as the de novo synthesis and deposition of ECM contribute to the reparative second phase after clearing of damaged cells and ECM. In addition to strongly decreased inflammation, *Has2* KO hearts are characterized by reduced α-SMA–positive fibroblasts in the infarct and border zones. The current results suggest that this is not due to increased fibroblast apoptosis but instead due to decreased myofibroblastic differentiation and proliferation.

TGF-β1 is a well-recognized regulator of fibroblast and myofibroblast function, for example, during wound healing, and of the orchestration of ECM organization and homeostasis in noncardiac tissues. Less is known in the heart after AMI,[33] but TGF-β1 is likely crucial for the myofibroblast response after cardiac I/R. Of note, TGF-β1 can exert both beneficial

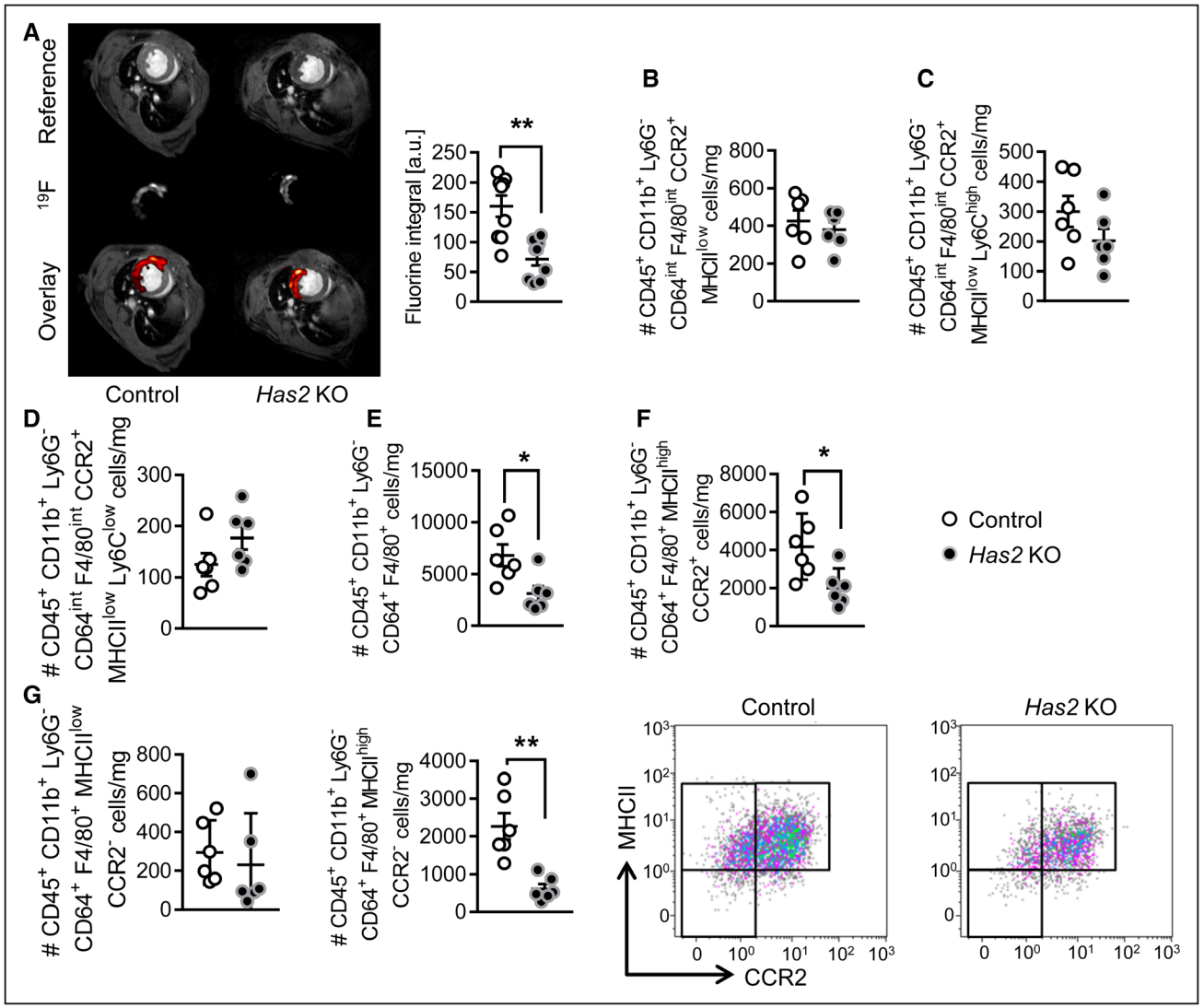

Figure 6. Reduced cardiac macrophages in *Has2* KO (Has2 deficient) mice 72 h post-ischemia and reperfusion. A, Representative midventricular short-axis images and quantification of inflammatory cells by ^{19}F MRI (magnetic resonance imaging) in *Has2* KO mice vs control, n=9, 9. **B–D**, Detailed cardiac immune cell analyses by flow cytometric measurements showing (**B**) unaltered total monocytes (MHCII^{low}CCR2^{+}), n=6, 6, as well as (**C**) Ly6C^{high}, n=6, 6 and (**D**) Ly6C^{low} subsets, n=6, 6, and reduced amounts of (**E**) total macrophages (F4/80^{+}CD64^{+}), n=6, 6, (**F**) monocyte-derived macrophages (MHCII^{high}CCR2^{+}), n=6, 6, and (**G**) resident (MHCII$^{high\ or\ low}$CCR2^{-}) macrophages, n=6, 6, and respective representative plots. Data represent mean±SEM; *P<0.05, **P<0.01. CCR2 indicates C-C chemokine receptor type 2; CD, cluster of differentiation; and MHCII, major histocompatibility complex II.

and detrimental effects.[33] Whereas early inhibition of TGF-β1 impaired the outcome after experimental AMI,[34] inhibition in the subacute phase reduced adverse cardiac remodeling.[35] Here, we observed in cardiac fibroblasts after blocking of the HA receptor CD44 in vitro inhibition of TGF-β1–specific responses such as reduced SMAD2 phosphorylation and reduced α-SMA expression. These findings strongly suggest that HA-mediated signaling through CD44 promotes activation of TGF-β1 signal transduction in cardiac fibroblasts. SMAD2 phosphorylation has been used as readout for activation of TGF-β1 signaling. This is in line with reduced numbers of myofibroblasts after I/R in *Has2* KO mice. It has been demonstrated that CD44 contributes to TGF-mediated SMAD phosphorylation in fibroblasts and cancer cells[36,37] and that CD44 cooperates with epidermal growth factor receptor in enhancing TGF-β1–mediated fibroblast activation.[38] TGF-β1 also activates noncanonical SMAD-independent signaling pathways including ERK and PI3K (phosphoinositide 3-kinase)[39] that were also addressed in the present study. Both have been shown to contribute to fibroblast activation.[39] The present data in *Has2* KOs and experiments blocking of CD44, however, do not allow the conclusion that SMAD2 phosphorylation itself is critical for the observed phenotype. SMAD3 and noncanonical TGF-β1 signaling cascades may be considered in detail in future studies. SMAD3 is a promising candidate for further studies and has been attributed an important role in modulating the myofibroblast phenotype after I/R, especially regarding the control of fibroblast proliferation, scar remodeling, collagen synthesis, and cellular alignment in the infarct but not α-SMA expression[40] as altered in *Has2* KOs.

TGF-β1 also regulates monocyte/macrophage-mediated inflammation. It activates monocytes and inhibits macrophages and thereby contributes to the temporal and spatial fine-tuning of inflammation and wound healing.[33] Evidence

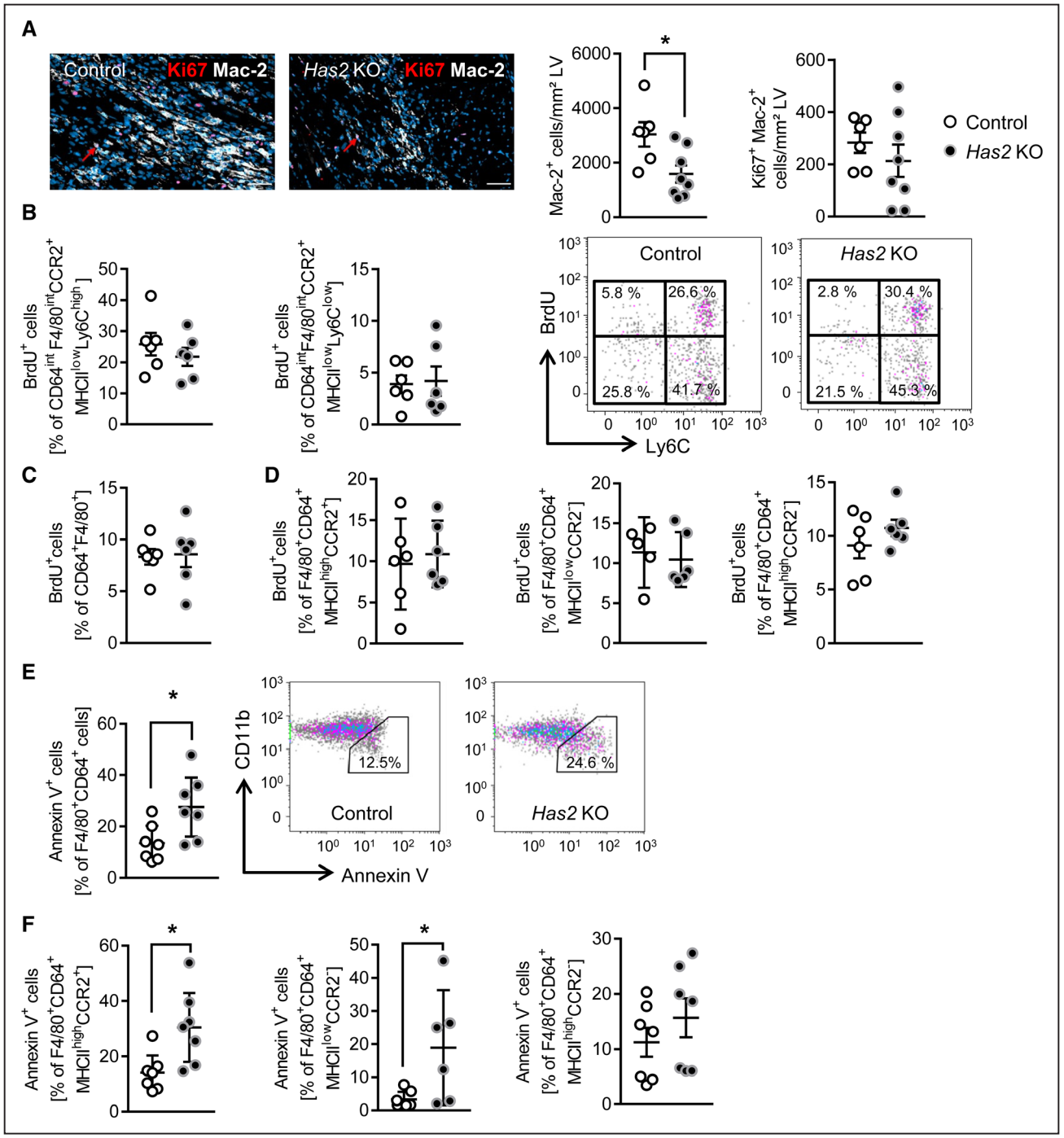

Figure 7. Increased cardiac macrophage apoptosis in *Has2* KO (*Has* deficient) mice 72 h post-ischemia and reperfusion (I/R). A, Immunohistochemical staining of Ki67 and Mac-2/Galectin-3 (**left**) and respective quantification (**right**) 72 h post-I/R in the total left ventricle (LV); scale bar indicates 50 µm, n=6, 8. Flow cytometric measurements of (**B**) BrdU^{+}Ly6C^{high} and ^{low} cardiac monocytes (**left**), n=6, 6, n=6, 6 and representative plots (**right**), (**C**) BrdU^{+} total CD64^{+}/F4/80^{+} macrophages, n=6, 6, (**D**) monocyte-derived (MHCII^{high}CCR2^{+}) n=6, 6, and resident (MHCII^{low} and ^{high}CCR2^{-}) macrophages, n=5, 6, n=6, 6. Numbers of annexin V–positive (**E**) total macrophages (F4/80^{+}CD64^{+}), with representative plots (**right**), n=7, 7, (**F**) monocyte-derived macrophages (MHCII^{high}CCR2^{+}), n=7, 7, and resident macrophages (MHCII^{low}CCR2), n=7, 6, and (MHCII^{high}CCR2^{-}) n=7, 7. Data represent mean±SEM; *P<0.05. BrdU indicates 5-bromo-2'-deoxyuridine; CCR2, C-C chemokine receptor type 2; CD, cluster of differentiation; and MHCII, major histocompatibility complex II.

suggests that both initial activation of inflammatory response and subsequent suppression of inflammation and the stimulation of reparative programs by TGF-β1 are an important part in orchestration of the different phases of cardiac healing after I/R.[41,42] However, the precise functions of TGF-β1 in inflammation await further experimentation. Therefore, the observed interference between the early HA-rich microenvironment after I/R and the modulation of TGF-β1 responses by CD44 in fibroblasts could also extend to monocytes/macrophages. All considered, we hypothesize that the loss of HAS2 leads to reduced HA/CD44 signaling that in turn impairs myofibroblastic differentiation and function.

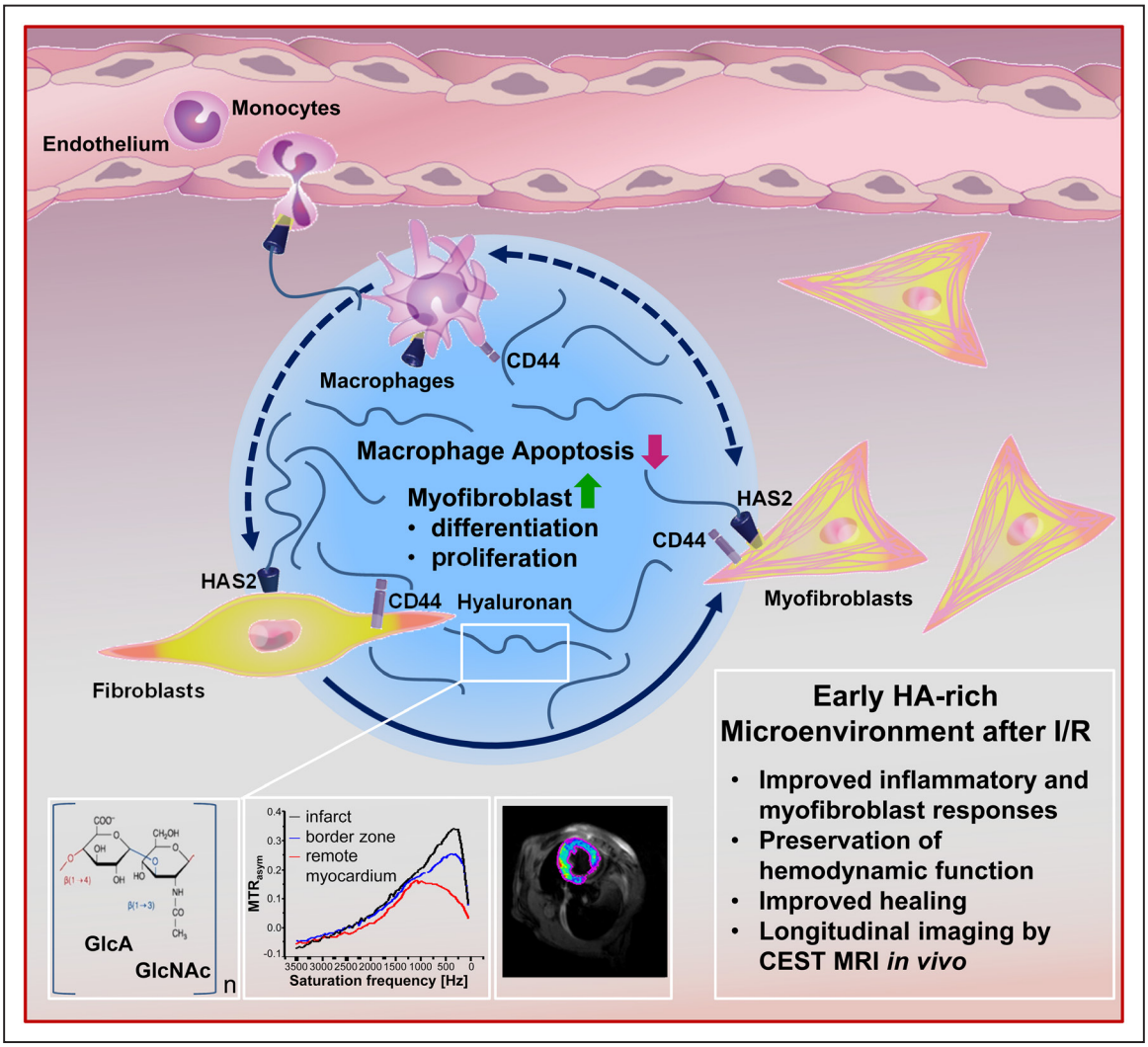

Figure 8. Schematic overview. Hyaluronan (HA) is a polymeric carbohydrate composed of alternating disaccharides of D-glucuronic acid-β-1, 3-N-acetylglucosamine-β-1, 4. A HA-rich microenvironment is rapidly formed by induction of HAS (HA synthase) 2 in cardiac fibroblasts after ischemia/reperfusion injury (I/R). In vitro experiments raised first evidence that monocytes/macrophages may contribute to de novo synthesis of HA. Experiments in *Has* KO (*Has2* deficient) mice showed that reduced cardiac HA after I/R leads to decreased numbers of monocyte-derived macrophages and resident macrophages because of increased macrophage apoptosis. Conversely, it is concluded that the HA-rich microenvironment protects macrophages from apoptosis. Potential mechanisms include CD (cluster of differentiation) 44-mediated activation of PI3K (phosphoinositide 3-kinase) signaling. In addition, deletion of *Has2* impaired myofibroblast differentiation after I/R and, as shown in vitro, impaired contractile and proliferative myofibroblast functions suggesting an important role of endogenous cardiac HA in myofibroblast phenotype. Mechanistically, HA/CD44 interactions activate TGF (transforming growth factor)-β/SMAD2 (mothers against decapentaplegic homolog 2) signaling in cardiac fibroblasts. The cross talk (dotted arrows) between macrophages and fibroblasts/myofibroblasts increases HA synthesis, promotes myofibroblast function, and protects macrophages from apoptosis. The current findings suggest that the decreased macrophage and myofibroblast response in *Has2* KO mice impairs infarct healing and thereby hemodynamic function. Conversely, the rapidly forming HA-rich microenvironment after I/R appears to be an endogenous repair mechanism. Because HA is highly hydroxylated containing numerous water exchangeable protons, it was possible to apply chemical exchange saturation transfer (CEST) magnetic resonance imaging (MRI) to visualize and quantify cardiac HA after I/R.

These results and conclusions are in line with data in *Cd44* KO mice showing ventricular dilatation, decreased fibroblast response and decreased fibroblast proliferation, and collagen synthesis.[43] Moreover, it has been reported that the addition of HA promotes the contraction of collagen gels by myofibroblasts compared with collagen gels without HA.[44] In support of the assumption that CD44 fine-tunes the functional phenotype of cardiac fibroblasts, is our recent finding that IL-6 induces HA synthesis in cardiac fibroblasts. This in turn activates CD44 resulting in stimulation of cytokine release by fibroblasts.[21] Furthermore, stimulation of cytokine release by HA/CD44 representing the proinflammatory fibroblast phenotype might connect the 2 observations made here that inhibition of HA synthesis in acute I/R causes both inhibition of macrophage-mediated inflammation and fibroblast activation.

It is shown here that in myocardial infarction, endogenous HA regulates the macrophage response. The impaired macrophage response likely contributes to the aggravated phenotype after I/R in *Has2* KOs. There is ample evidence in the literature that HA modulates inflammatory responses by a variety of mechanisms including stimulation of TLRs (Toll-like receptors) and providing an adhesive matrix for macrophages.[18] Another facet of HA in inflammation is its promoting effect on Th1 cell polarization that contributes to inflammation in

autoimmunity and atherosclerosis.[13] On the contrary, from studies in atherosclerosis, it is known that inhibition of HA synthesis impairs the endothelial glycocalyx, thereby facilitating adhesion and extravasation of monocytes and augmenting macrophage-driven inflammation and atheroprogression.[45] The observed phenotype in *Has2* KO mice after I/R was very specific for cardiac immune cells because immune cells in all other compartments such as bone marrow, blood, and spleen were unaffected. The effect was also specific for cardiac macrophages because lymphocytes, neutrophils, and even monocytes were unchanged by *Has2* deletion. The decrease in cardiac macrophages was driven by decreased numbers of $MHCII^{high}CCR2^{+}$ monocyte-derived macrophages but also detected in resident $MHCII^{high}CCR2^{-}$ macrophages. In general, MHCII-expressing macrophages ($CCR2^{+}$ and $CCR2^{-}$) are important coordinators of cardiac inflammation and crucial for antigen presentation.[46] Further, $CCR2^{+}$ macrophages, not only monocyte-derived but also including resident macrophages, are known to be crucially involved in the immune response post-cardiac ischemia.[47,48] Resident macrophages contribute to the repair response post-myocardial infarction.[49] Particularly, the MHC^{low} subset has been described to be important for the removal of dead cells[46] but also to trigger the recruitment of other immune cells such as neutrophils and monocytes to the heart after injury.[48] Because of these complex and divergent functions of cardiac macrophage subsets, experimental approaches to target those cells resulted in contrary effects on the functional outcome dependent on which cell type was mainly affected: inhibition of monocyte influx and thereby subsequent decrease in cardiac $CCR2^{+}$ macrophage content showed beneficial effects and reduced adverse remodeling and inhibited heart failure.[47,50] In contrast, broader approaches targeting all macrophages or also a reduction in resident macrophages showed opposite effects.[51]

Macrophage proliferation was not affected and the differentiation of monocytes into macrophages, based on in vitro results, was also independent of *Has2* deletion. However, apoptosis of cardiac macrophages after I/R was increased in *Has2* KO mice. Moreover, in vitro inhibition of HA synthesis and blocking CD44 also induced apoptosis in bone marrow–derived macrophages suggesting that the HA matrix present post-infarction augments the macrophage response by creating an antiapoptotic microenvironment. Antiapoptotic effects of CD44 have been reported in fibroblasts and malignant cells.[52] Further, a recent study showed that CD44/HA binding is critical for the survival of monocyte-derived alveolar macrophages by promoting HA binding and thereby a protective HA coat.[53] Interestingly, phosphorylation of AKT was reduced in vivo in *Has2* KO mice. It might, therefore, be considered that reduction of AKT signaling, which is in line with decreased macrophage apoptosis, might be caused by reduced CD44 signaling in macrophages. Indeed, CD44 has been shown to activate PI3K in macrophages, and phosphorylation of AKT inhibits macrophage apoptosis.[54] However, the role of HA/CD44 for macrophage apoptosis after cardiac I/R and the possible involvement of TGF-β1 signaling remains an important question for future studies.

In addition, the present results hint toward the contribution of a simple but possibly important mechanism that is based on instructive interactions between fibroblasts and monocyte/macrophages. It is shown here that monocytes/macrophages promote myofibroblastic differentiation in line with previous findings that cardiac fibroblasts support the transition of monocytes into macrophages and that fibroblasts protect macrophages from apoptosis. Thereby, the two effects namely reduction in macrophages and reduction in myofibroblasts might enforce each other and thereby aggravate the healing defect in *Has2* KO hearts. The main findings and conclusions are schematically depicted in Figure 8.

Whereas determination of the properties of myocardial tissue and the extracellular volume by MRI using T1/T2 mapping and gadolinium enhancement is feasible and may be used for classification of disease stages,[55] it is, however, desirable to visualize and discriminate specific pathophysiologic processes after myocardial infarction. For this purpose, molecular imaging techniques that allow the visualization of specific molecular patterns have been developed in other preclinical studies.[56] To date, in cardiac imaging of the ECM post-myocardial infarction, it was attempted to visualize cardiac collagen or collagen degradation by MMPs. Cardiac collagen is associated with cardiac maladaptation and cardiac fibrosis leading to stiffening and hemodynamic dysfunction. Thereby, cardiac collagen is a marker of the relatively late phase in the (mal)adaptation to I/R. As shown here, HA matrix is likely the first cell-derived matrix that is elaborated post-I/R injury. Increased cellular fibronectin deposition has also been shown after 24 hours but continues to rise during a period of 7 days,[20] whereas *Has1* and *Has2* expression peak at 6 and 48 hours after I/R suggesting that the HA response is very concise (Online Figure I). To address the early remodeling, we present here a CEST MRI method to image the provisional HA matrix after I/R by combining the CEST approach with black blood adjustment. CEST MRI clearly visualized the HA response within the first 72 hours after I/R as proved by the suppression of the CEST signal by 4-MU and in *Has2* KO mice. Introduction of a black blood preparation before the saturation transfer avoided potential contaminations from CEST-active components in the blood (in particular sugars and glycosylated proteins) and enhanced the specificity of the approach for imaging of the HA matrix. This allowed the sensitive detection of alterations in magnetization transfer ratio asymmetry images already 24 hours after I/R, which has not been reported before.

In conclusion, the current data show that cell-mediated HA synthesis by HAS2 is an acute response to cardiac ischemia, which is indispensable for proper macrophage and fibroblast responses and thereby crucial for infarct healing. Cardiac HA may be a promising prognostic marker or therapeutic target in the acute phase post-I/R because of the rapid onset of cardiac HA synthesis and its functional importance for fibroblast and immune responses.

Acknowledgments

We wish to acknowledge Petra Rompel and Kerstin Freidel for technical support.

Sources of Funding

This study was supported by Deutsche Forschungsgemeinschaft, SFB 1116.

Disclosures

None.

References

1. Roe MT, Messenger JC, Weintraub WS, Cannon CP, Fonarow GC, Dai D, Chen AY, Klein LW, Masoudi FA, McKay C, Hewitt K, Brindis RG, Peterson ED, Rumsfeld JS. Treatments, trends, and outcomes of acute myocardial infarction and percutaneous coronary intervention. *J Am Coll Cardiol*. 2010;56:254–263.
2. Moran AE, Forouzanfar MH, Roth GA, Mensah GA, Ezzati M, Flaxman A, Murray CJ, Naghavi M. The global burden of ischemic heart disease in 1990 and 2010: the Global Burden of Disease 2010 study. *Circulation*. 2014;129:1493–1501. doi: 10.1161/CIRCULATIONAHA.113.004046
3. Kloner RA. Current state of clinical translation of cardioprotective agents for acute myocardial infarction. *Circ Res.* 2013;113:451–463. doi: 10.1161/CIRCRESAHA.112.300627
4. Ibáñez B, Heusch G, Ovize M, Van de Werf F. Evolving therapies for myocardial ischemia/reperfusion injury. *J Am Coll Cardiol.* 2015;65:1454–1471. doi: 10.1016/j.jacc.2015.02.032
5. Li AH, Liu PP, Villarreal FJ, Garcia RA. Dynamic changes in myocardial matrix and relevance to disease: translational perspectives. *Circ Res.* 2014;114:916–927. doi: 10.1161/CIRCRESAHA.114.302819
6. Frangogiannis NG. The extracellular matrix in myocardial injury, repair, and remodeling. *J Clin Invest.* 2017;127:1600–1612. doi: 10.1172/JCI87491
7. Prabhu SD, Frangogiannis NG. The biological basis for cardiac repair after myocardial infarction: from inflammation to fibrosis. *Circ Res.* 2016;119:91–112. doi: 10.1161/CIRCRESAHA.116.303577
8. Swirski FK, Nahrendorf M, Etzrodt M, Wildgruber M, Cortez-Retamozo V, Panizzi P, Figueiredo JL, Kohler RH, Chudnovskiy A, Waterman P, Aikawa E, Mempel TR, Libby P, Weissleder R, Pittet MJ. Identification of splenic reservoir monocytes and their deployment to inflammatory sites. *Science.* 2009;325:612–616. doi: 10.1126/science.1175202
9. Frangogiannis NG. Emerging roles for macrophages in cardiac injury: cytoprotection, repair, and regeneration. *J Clin Invest.* 2015;125:2927–2930. doi: 10.1172/JCI83191
10. Alex L, Frangogiannis NG. The Cellular Origin of Activated Fibroblasts in the Infarcted and Remodeling Myocardium. *Circ Res.* 2018;122:540–542. doi: 10.1161/CIRCRESAHA.118.312654
11. Barallobre-Barreiro J, Didangelos A, Schoendube FA, Drozdov I, Yin X, Fernández-Caggiano M, Willeit P, Puntmann VO, Aldama-López G, Shah AM, Doménech N, Mayr M. Proteomics analysis of cardiac extracellular matrix remodeling in a porcine model of ischemia/reperfusion injury. *Circulation.* 2012;125:789–802. doi: 10.1161/CIRCULATIONAHA.111.056952
12. Kiene LS, Homann S, Suvorava T, et al. Deletion of hyaluronan synthase 3 inhibits neointimal hyperplasia in mice. *Arterioscler Thromb Vasc Biol.* 2016;36:e9–e16. doi: 10.1161/ATVBAHA.115.306607
13. Homann S, Grandoch M, Kiene LS, Podsvyadek Y, Feldmann K, Rabausch B, Nagy N, Lehr S, Kretschmer I, Oberhuber A, Bollyky P, Fischer JW. Hyaluronan synthase 3 promotes plaque inflammation and atheroprogression. *Matrix Biol.* 2018;66:67–80. doi: 10.1016/j.matbio.2017.09.005
14. Nagy N, Kaber G, Johnson PY, Gebe JA, Preisinger A, Falk BA, Sunkari VG, Gooden MD, Vernon RB, Bogdani M, Kuipers HF, Day AJ, Campbell DJ, Wight TN, Bollyky PL. Inhibition of hyaluronan synthesis restores immune tolerance during autoimmune insulitis. *J Clin Invest.* 2015;125:3928–3940. doi: 10.1172/JCI79271
15. Fischer JW. Role of hyaluronan in atherosclerosis: current knowledge and open questions [published online March 3, 2018]. *Matrix Biol*. https://doi.org/10.1016/j.matbio.2018.03.003
16. Aya KL, Stern R. Hyaluronan in wound healing: rediscovering a major player. *Wound Repair Regen.* 2014;22:579–593. doi: 10.1111/wrr.12214
17. Camenisch TD, Schroeder JA, Bradley J, Klewer SE, McDonald JA. Heart-valve mesenchyme formation is dependent on hyaluronan-augmented activation of ErbB2-ErbB3 receptors. *Nat Med.* 2002;8:850–855. doi: 10.1038/nm742
18. Grandoch M, Bollyky PL, Fischer JW. Hyaluronan: a master switch between vascular homeostasis and inflammation. *Circ Res.* 2018;122:1341–1343. doi: 10.1161/CIRCRESAHA.118.312522
19. Camenisch TD, Spicer AP, Brehm-Gibson T, Biesterfeldt J, Augustine ML, Calabro A Jr, Kubalak S, Klewer SE, McDonald JA. Disruption of hyaluronan synthase-2 abrogates normal cardiac morphogenesis and hyaluronan-mediated transformation of epithelium to mesenchyme. *J Clin Invest.* 2000;106:349–360. doi: 10.1172/JCI10272
20. Dobaczewski M, Bujak M, Zymek P, Ren G, Entman ML, Frangogiannis NG. Extracellular matrix remodeling in canine and mouse myocardial infarcts. *Cell Tissue Res.* 2006;324:475–488. doi: 10.1007/s00441-005-0144-6
21. Müller J, Gorressen S, Grandoch M, Feldmann K, Kretschmer I, Lehr S, Ding Z, Schmitt JP, Schrader J, Garbers C, Heusch G, Kelm M, Scheller J, Fischer JW. Interleukin-6-dependent phenotypic modulation of cardiac fibroblasts after acute myocardial infarction. *Basic Res Cardiol.* 2014;109:440. doi: 10.1007/s00395-014-0440-y
22. Seibler J, Zevnik B, Küter-Luks B, Andreas S, Kern H, Hennek T, Rode A, Heimann C, Faust N, Kauselmann G, Schoor M, Jaenisch R, Rajewsky K, Kühn R, Schwenk F. Rapid generation of inducible mouse mutants. *Nucleic Acids Res.* 2003;31:e12.
23. Matsumoto K, Li Y, Jakuba C, Sugiyama Y, Sayo T, Okuno M, Dealy CN, Toole BP, Takeda J, Yamaguchi Y, Kosher RA. Conditional inactivation of Has2 reveals a crucial role for hyaluronan in skeletal growth, patterning, chondrocyte maturation and joint formation in the developing limb. *Development*. 2009;136:2825–2835. doi: 10.1242/dev.038505
24. Chan DD, Xiao WF, Li J, de la Motte CA, Sandy JD, Plaas A. Deficiency of hyaluronan synthase 1 (Has1) results in chronic joint inflammation and widespread intra-articular fibrosis in a murine model of knee joint cartilage damage. *Osteoarthritis Cartilage.* 2015;23:1879–1889. doi: 10.1016/j.joca.2015.06.021
25. Merx MW, Gorressen S, van de Sandt AM, Cortese-Krott MM, Ohlig J, Stern M, Rassaf T, Gödecke A, Gladwin MT, Kelm M. Depletion of circulating blood NOS3 increases severity of myocardial infarction and left ventricular dysfunction. *Basic Res Cardiol.* 2014;109:398. doi: 10.1007/s00395-013-0398-1
26. Nossuli TO, Lakshminarayanan V, Baumgarten G, Taffet GE, Ballantyne CM, Michael LH, Entman ML. A chronic mouse model of myocardial ischemia-reperfusion: essential in cytokine studies. *Am J Physiol Heart Circ Physiol.* 2000;278:H1049–H1055. doi: 10.1152/ajpheart.2000.278.4.H1049
27. Flögel U, Ding Z, Hardung H, Jander S, Reichmann G, Jacoby C, Schubert R, Schrader J. In vivo monitoring of inflammation after cardiac and cerebral ischemia by fluorine magnetic resonance imaging. *Circulation.* 2008;118:140–148. doi: 10.1161/CIRCULATIONAHA.107.737890
28. Temme S, Grapentin C, Quast C, Jacoby C, Grandoch M, Ding Z, Owenier C, Mayenfels F, Fischer JW, Schubert R, Schrader J, Flögel U. Noninvasive imaging of early venous thrombosis by 19F magnetic resonance imaging with targeted perfluorocarbon nanoemulsions. *Circulation.* 2015;131:1405–1414. doi: 10.1161/CIRCULATIONAHA.114.010962
29. Haberkorn SM, Jacoby C, Ding Z, Keul P, Bonner F, Polzin A, Levkau B, Schrader J, Kelm M, Flogel U. Cardiovascular magnetic resonance relaxometry predicts regional functional outcome after experimental myocardial infarction. *Circ Cardiovasc Imaging*. 2017;10:e006025.
30. Westermann D, Mersmann J, Melchior A, et al. Biglycan is required for adaptive remodeling after myocardial infarction. *Circulation.* 2008;117:1269–1276. doi: 10.1161/CIRCULATIONAHA.107.714147
31. Ling W, Regatte RR, Navon G, Jerschow A. Assessment of glycosaminoglycan concentration in vivo by chemical exchange-dependent saturation transfer (gagcest). *Proc Natl Acad Sci USA*. 2008;105:2266–2270.
32. van Zijl PC, Yadav NN. Chemical exchange saturation transfer (CEST): what is in a name and what isn't? *Magn Reson Med.* 2011;65:927–948. doi: 10.1002/mrm.22761
33. Frangogiannis NG. The role of transforming growth factor (TGF)-β in the infarcted myocardium. *J Thorac Dis.* 2017;9:S52–S63. doi: 10.21037/jtd.2016.11.19
34. Frantz S, Hu K, Adamek A, Wolf J, Sallam A, Maier SK, Lonning S, Ling H, Ertl G, Bauersachs J. Transforming growth factor beta inhibition increases mortality and left ventricular dilatation after myocardial infarction. *Basic Res Cardiol.* 2008;103:485–492. doi: 10.1007/s00395-008-0739-7
35. Okada H, Takemura G, Kosai K, Li Y, Takahashi T, Esaki M, Yuge K, Miyata S, Maruyama R, Mikami A, Minatoguchi S, Fujiwara T, Fujiwara H. Postinfarction gene therapy against transforming growth factor-beta signal modulates infarct tissue dynamics and attenuates left ventricular remodeling and heart failure. *Circulation.* 2005;111:2430–2437. doi: 10.1161/01.CIR.0000165066.71481.8E
36. Meran S, Thomas DW, Stephens P, Enoch S, Martin J, Steadman R, Phillips AO. Hyaluronan facilitates transforming growth factor-beta1-mediated fibroblast proliferation. *J Biol Chem.* 2008;283:6530–6545. doi: 10.1074/jbc.M704819200

37. Bourguignon LY, Singleton PA, Zhu H, Zhou B. Hyaluronan promotes signaling interaction between CD44 and the transforming growth factor beta receptor I in metastatic breast tumor cells. *J Biol Chem.* 2002;277:39703–39712. doi: 10.1074/jbc.M204320200
38. Midgley AC, Rogers M, Hallett MB, Clayton A, Bowen T, Phillips AO, Steadman R. Transforming growth factor-β1 (TGF-β1)-stimulated fibroblast to myofibroblast differentiation is mediated by hyaluronan (HA)-facilitated epidermal growth factor receptor (EGFR) and CD44 co-localization in lipid rafts. *J Biol Chem.* 2013;288:14824–14838. doi: 10.1074/jbc.M113.451336
39. Derynck R, Zhang YE. Smad-dependent and Smad-independent pathways in TGF-beta family signalling. *Nature.* 2003;425:577–584. doi: 10.1038/nature02006
40. Kong P, Shinde AV, Su Y, Russo I, Chen B, Saxena A, Conway SJ, Graff JM, Frangogiannis NG. Opposing actions of fibroblast and cardiomyocyte Smad3 signaling in the infarcted myocardium. *Circulation.* 2018;137:707–724. doi: 10.1161/CIRCULATIONAHA.117.029622
41. Birdsall HH, Green DM, Trial J, Youker KA, Burns AR, MacKay CR, LaRosa GJ, Hawkins HK, Smith CW, Michael LH, Entman ML, Rossen RD. Complement C5a, TGF-beta 1, and MCP-1, in sequence, induce migration of monocytes into ischemic canine myocardium within the first one to five hours after reperfusion. *Circulation.* 1997;95:684–692.
42. Xiao YQ, Freire-de-Lima CG, Janssen WJ, Morimoto K, Lyu D, Bratton DL, Henson PM. Oxidants selectively reverse TGF-beta suppression of proinflammatory mediator production. *J Immunol.* 2006;176:1209–1217.
43. Huebener P, Abou-Khamis T, Zymek P, Bujak M, Ying X, Chatila K, Haudek S, Thakker G, Frangogiannis NG. CD44 is critically involved in infarct healing by regulating the inflammatory and fibrotic response. *J Immunol.* 2008;180:2625–2633.
44. Travis JA, Hughes MG, Wong JM, Wagner WD, Geary RL. Hyaluronan enhances contraction of collagen by smooth muscle cells and adventitial fibroblasts: role of CD44 and implications for constrictive remodeling. *Circ Res.* 2001;88:77–83.
45. Nagy N, Freudenberger T, Melchior-Becker A, Röck K, Ter Braak M, Jastrow H, Kinzig M, Lucke S, Suvorava T, Kojda G, Weber AA, Sörgel F, Levkau B, Ergün S, Fischer JW. Inhibition of hyaluronan synthesis accelerates murine atherosclerosis: novel insights into the role of hyaluronan synthesis. *Circulation.* 2010;122:2313–2322. doi: 10.1161/CIRCULATIONAHA.110.972653
46. Epelman S, Lavine KJ, Beaudin AE, et al. Embryonic and adult-derived resident cardiac macrophages are maintained through distinct mechanisms at steady state and during inflammation. *Immunity.* 2014;40:91–104. doi: 10.1016/j.immuni.2013.11.019
47. Sager HB, Hulsmans M, Lavine KJ, et al. Proliferation and recruitment contribute to myocardial macrophage expansion in chronic heart failure. *Circ Res.* 2016;119:853–864. doi: 10.1161/CIRCRESAHA.116.309001
48. Li W, Hsiao HM, Higashikubo R, Saunders BT, Bharat A, Goldstein DR, Krupnick AS, Gelman AE, Lavine KJ, Kreisel D. Heart-resident ccr2(+) macrophages promote neutrophil extravasation through tlr9/myd88/cxcl5 signaling. *JCI Insight*. 2016;1:e87315.
49. Lavine KJ, Epelman S, Uchida K, Weber KJ, Nichols CG, Schilling JD, Ornitz DM, Randolph GJ, Mann DL. Distinct macrophage lineages contribute to disparate patterns of cardiac recovery and remodeling in the neonatal and adult heart. *Proc Natl Acad Sci USA*. 2014;111:16029–16034.
50. Kaikita K, Hayasaki T, Okuma T, Kuziel WA, Ogawa H, Takeya M. Targeted deletion of CC chemokine receptor 2 attenuates left ventricular remodeling after experimental myocardial infarction. *Am J Pathol.* 2004;165:439–447. doi: 10.1016/S0002-9440(10)63309-3
51. van Amerongen MJ, Harmsen MC, van Rooijen N, Petersen AH, van Luyn MJ. Macrophage depletion impairs wound healing and increases left ventricular remodeling after myocardial injury in mice. *Am J Pathol.* 2007;170:818–829. doi: 10.2353/ajpath.2007.060547
52. Fujita Y, Kitagawa M, Nakamura S, Azuma K, Ishii G, Higashi M, Kishi H, Hiwasa T, Koda K, Nakajima N, Harigaya K. CD44 signaling through focal adhesion kinase and its anti-apoptotic effect. *FEBS Lett.* 2002;528:101–108.
53. Dong Y, Poon GFT, Arif AA, Lee-Sayer SSM, Dosanjh M, Johnson P. The survival of fetal and bone marrow monocyte-derived alveolar macrophages is promoted by CD44 and its interaction with hyaluronan. *Mucosal Immunol.* 2018;11:601–614. doi: 10.1038/mi.2017.83
54. Babaev VR, Ding L, Zhang Y, May JM, Lin PC, Fazio S, Linton MF. Macrophage IKKα deficiency suppresses Akt phosphorylation, reduces cell survival, and decreases early atherosclerosis. *Arterioscler Thromb Vasc Biol.* 2016;36:598–607. doi: 10.1161/ATVBAHA.115.306931
55. Parsai C, O'Hanlon R, Prasad SK, Mohiaddin RH. Diagnostic and prognostic value of cardiovascular magnetic resonance in non-ischaemic cardiomyopathies. *J Cardiovasc Magn Reson.* 2012;14:54. doi: 10.1186/1532-429X-14-54
56. de Haas HJ, Arbustini E, Fuster V, Kramer CM, Narula J. Molecular imaging of the cardiac extracellular matrix. *Circ Res.* 2014;114:903–915. doi: 10.1161/CIRCRESAHA.113.302680